3rd URSI AT-AP-RASC, Gran Canaria, 29 May – 3 June 2022

Physics informed neural network (PINN) for noise-robust phase-based magnetic resonance electrical properties tomography

Adan J. Garcia Inda*(1), Shao Y. Huang(2)(3), Nevrez Immamoglu(4) and Wenwei Yu(1)(5)
(1) Department of Medical Engineering, Chiba University, Chiba, Japan
(2) Department of Surgery, National University of Singapore, Singapore, Singapore
(3) Engineering Product Development Department, Singapore University of Technology and Design, Singapore, Singapore
(4) Digital Architecture Research Center, National Institute of Advanced Industrial Science and Technology, Tokyo, Japan
(5) Center for Frontier Medical Engineering, Chiba University, Chiba, Japan

Abstract

Electrical properties could become a source of contrast for non-calcified tumor tissues. Magnetic Resonance Electrical Property Tomography (MREPT) relies on numerical differentiation to solve the partial differential equations (PDEs) to reconstruct electrical properties. However, the numerical differentiation for derivatives produces artifacts near tissue edges and amplifies noise. In this work, Physics-informed neural networks (PINNs), are employed to estimate derivatives for MREPT with automatic differentiation enabled by neural networks to improve noise robustness and reduce edge artifacts. PINNs require the balance of various loss functions and information from collocation points of ground truth and image boundary to learn to estimate the derivatives. In this work, a warm-up mechanism is used to reduce the complexity of the multiple loss balance. Results showed that even with only three collocation points and boundary conditions, reconstructions can be made from noise-contaminated source images (SNR 50). This proves that PINNs achieved noise-robust estimate of partial derivatives, thus leding to noise-robust conductivity reconstruction.

1 Introduction

Electrical properties are quantitative properties of biological tissues that could enhance the determination of non-calcified tumorous tissues [1]. Moreover, knowledge of electrical properties is a foundation to calculate specific absorption rate (SAR) for RF safety where humans are exposed to RF fields., e.g., wireless power transfer [2]. Magnetic resonance electrical properties tomography (MREPT) is a technique to reconstruct the conductivity of tissues from MRI measurements, the B_1 fields [3]. The reconstruction formulation is based on Maxwell's equations. To decrease scan time, conductivity focused formulations have been developed [4], in which, the MRI's phase sum of B_1^+ and B_1^- ($\varphi^+ + \varphi^-$), also known as the transceive phase (φ^{tr}) is used to reconstruct the conductivity of tissues. A common formulation for phase-based conductivity reconstruction is referred to as std-EPT. In std-EPT, the reconstructed conductivity is assumed to be homogeneous. While this assumption simplifies the reconstruction, it produces artifacts near tissue edges and is noise susceptible due to being based on the second-order partial derivative of the φ^{tr}. To reconstruct the conductivity without the homogeneity assumption, convection-reaction EPT (cr-EPT) was proposed [5]. The resulting convection-reaction partial differential equation (PDE) is discretized and solved as a set of linear equations. However, numerical instabilities appear in the solution associated with the discretization. A viscosity-type regularization term was introduced in [6], to dampen such numerical instabilities. Furthermore, a corresponding phase-based stabilized cr-EPT (stab-EPT) was proposed [4]. However, because the regularization term is set by experience it leads to undershooting of the reconstructed conductivity. MREPT's reconstruction of conductivity requires the numerical calculation of φ^{tr} spatial partial derivatives. Savitzky-Golay filter based derivative calculation [7] is an accurate method [6]. However, this method still suffers from erroneous values near tissue edges and is susceptible to noise. On the other hand, solvers of PDEs by data-driven Physics-informed neural networks (PINNs) have been proposed recently [8] to solve fluid simulation associated PDEs. PINNs are shown to efficiently solve multidimensional PDEs [9]. In PINNs, a neural network (NN) is trained to predict a field according to boundary conditions, and collocation points. Next, through automatic differentiation, spatial or temporal partial derivatives are estimated to solve a PDE. The residual of the PDE is added to the loss function. In this work, we propose a PINN method to predict conductivity values from noisy phase measurements. By applying phase-based MREPT formulations as constraints a framework for noise-robust conductivity reconstruction that overcomes current numerically-based formulations is created.

2 Methods

The canonical formulation for MREPT also known as the Helmholtz formulation [10] is shown as follows.

$$-\nabla^2 B_1^+ = \frac{\nabla \kappa}{\kappa} \times (\nabla \times B_1^+) - i\omega\mu_0 \kappa B_1^+ \qquad (1)$$

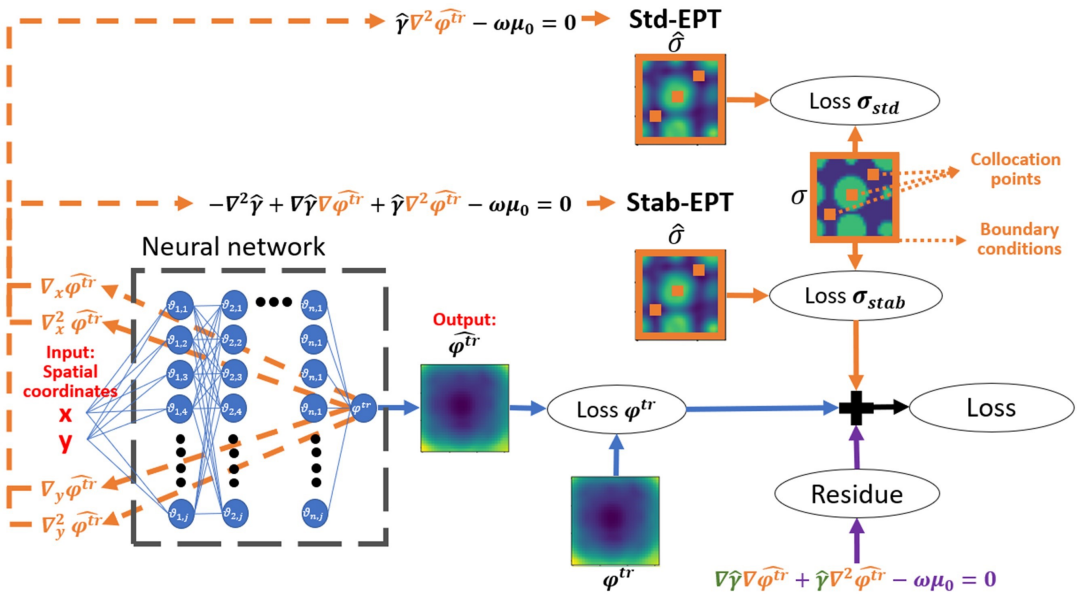

Figure 1. The neural network (NN) learns to predict the φ^{tr}, from the location values (x,y). φ^{tr} is backpropagated to the location values to estimate partial derivatives $\nabla\varphi^{\text{tr}}, \nabla^2\varphi^{\text{tr}}$. The partial derivatives are used to calculate the conductivity with Eq.2 and Eq.3. Lastly, the numerical derivative of φ^{tr} is calculated numerically to solve Eq.6 and added to the total loss function. The sum of the loss functions guide the conductivity reconstruction.

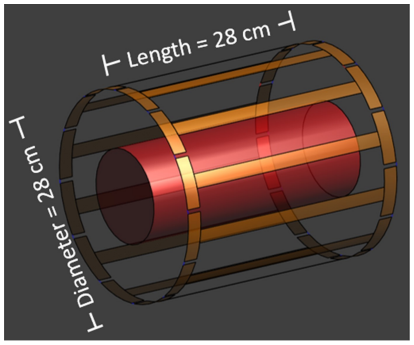

Figure 2. High-pass 16 rung birdcage coil in quadrature mode at 3T loaded with cylindrical phantom

where κ is the complex permittivity $(\frac{\sigma}{\omega\varepsilon_0} + i\varepsilon_r)$, σ is the conductivity in S/m, ε_r is the relative permittivity, ω is the frequency of the applied RF waves (i.e. B_1-fields), and B_1^+ is the RF field of transmit coils, $B_1^+ = B_x + iB_y$ [11]. The phase-based std-EPT method assumes homogeneity of the reconstructed conductivity to simplify the Helmholtz formulation as follows.

$$\gamma\nabla^2\varphi^{\text{tr}} = \omega\mu_0 \tag{2}$$

where γ is the inverse of the conductivity $(1/\sigma)$. This method relies uniquely on the calculation of the second order derivative, which makes it susceptible to noise. The phase-based cr-EPT formulation removes the homogeneity assumption to improve the reconstruction accuracy. The resulting formulation is as follows.

$$-\rho\nabla^2\gamma + \nabla\gamma\nabla\varphi^{\text{tr}} + \gamma\nabla^2\varphi^{\text{tr}} = \omega\mu_0 \tag{3}$$

where ρ is the coefficient of the viscosity-type regularization term. Although this formulation is more accurate than std-EPT, it still suffers from noise susceptibility. Fig. 1 shows a diagram for the proposed single case reconstruction method. A set of spatial coordinates (x,y) are input to a small NN, then the NN output is the predicted value of φ^{tr} at the corresponding spatial coordinates according to the data loss function below,

$$Loss_{\varphi^{\text{tr}}} = MSE(\varphi^{\text{tr}}, \hat{\varphi}^{\text{tr}}) \tag{4}$$

where MSE is the mean squared error function that measures the fidelity between the predicted $\hat{\varphi}^{\text{tr}}$ by the NN and φ^{tr} value from the measurement. Next, through automatic differentiation (backpropagation) [12], the partial derivatives with respect to the spatial values (x,y) are estimated according to the predicted $\hat{\varphi}^{\text{tr}}$. As the second-order derivatives are needed to reconstruct the conductivity, the results of the first backpropagation are summed and backpropagated once more to produce a second-order partial derivative $(\nabla^2\hat{\varphi}^{\text{tr}})$. With the partial derivatives, a conductivity map, $\hat{\sigma}$, can be constructed based the std-EPT formulation on Eq. 2, or the stab-EPT formulation on Eq. 3. With the reconstructed $\hat{\sigma}$, a second loss function is introduced to match boundary conditions and collocation points from the ground-truth conductivity (σ).

$$\begin{aligned} Loss_{\sigma} = {} & MSE(\sigma, \hat{\sigma}_{\text{std-EPT}}) \\ & + MSE(\sigma, \hat{\sigma}_{\text{stab-EPT}}) \end{aligned} \tag{5}$$

A two-pixel width Dirichlet boundary condition is applied around the periphery of the region of interest (ROI). And three pixels inside the ROI are selected as collocation points. Lastly, a PDE residual loss based on the Eq. 3 can

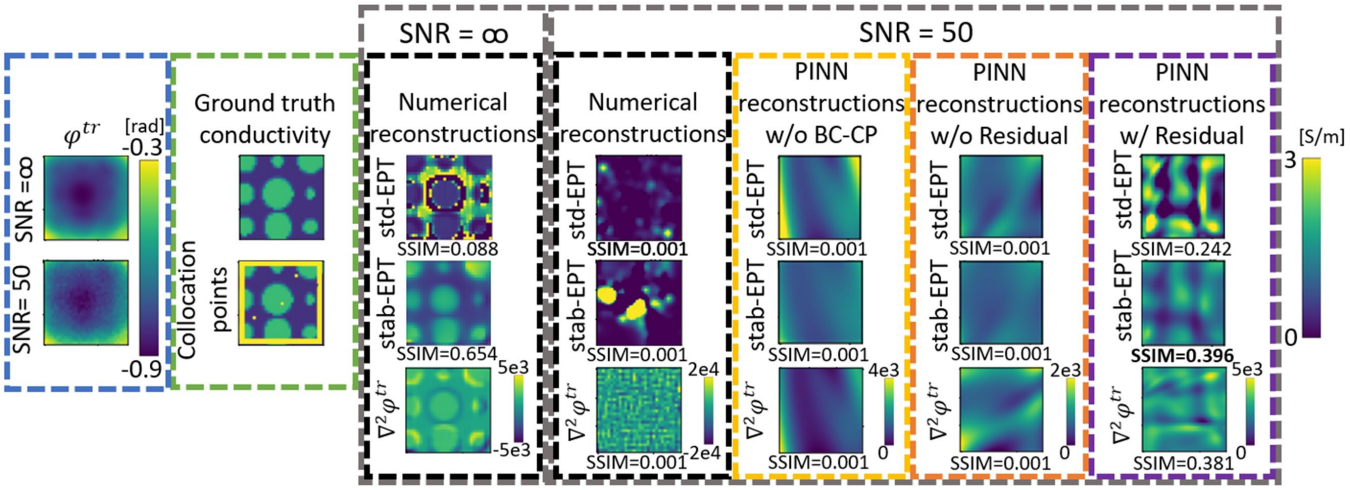

Figure 3. φ^{tr} from numerical experiment SNR = ∞, 50, ground truth conductivity with added boundary conditions (BC) and collocation points (CP) in yellow, 50 SNR reconstructions with numerical derivatives, 50 SNR reconstructions by PINN without BC-CP present, 50 SNR reconstructions without Helmholtz equation residue, and 50 SNR reconstructions by the proposed method PINN with Helmholtz equation residue.

be added according to the equation below,

$$Loss_{\mathbf{PDE}} = |\nabla\gamma\nabla\varphi^{\text{tr}} + \gamma\nabla^2\varphi^{\text{tr}} - \omega\mu_0| \tag{6}$$

The gradient of the predicted conductivity ($\nabla\gamma$) is numerically calculated through forward differences. This loss function serves as a direct guide for the NN to solve the PDE and decrease the degrees of freedom of the solution provided by the NN function. The loss functions terms are weighted and summed as it follows.

$$Loss = \lambda_1 Loss_{\varphi^{\text{tr}}} + \lambda_2 Loss_{\sigma} + \lambda_3 Loss_{\mathbf{PDE}} \tag{7}$$

For the test case, the weighting values are found empirically ($\lambda_1 = 200$, $\lambda_2 = 1$ and $\lambda_3 = 0.0008$) and minimized by modifying the NN's parameters according to "Adam" algorithm [7]. To maintain data fidelity to the phase measurement, a warm-up mechanism is adapted where for the first 10 thousand epochs $Loss_{\varphi^{\text{tr}}}$ is the only guiding force for the NN. The NN training took approximately 1 hour for 100 thousand epochs on a Nvidia GeForce RTX 2070 GPU card.

A numerical simulation is generated in Sim4Life© as a test case, composed of a binary-value cylinder phantom. The phantom is placed inside a high-pass 16 rung birdcage coil excited in quadrature mode at 3T. The coil dimensions are 14 cm radius and 28 cm length. The phantom inside the coil can be seen in Fig. 2. The 5 cm^2 φ^{tr} at the center of the coil is extracted and noise is added according to formulations in the literature [5]. The noise-contaminated φ^{tr} is use as the label for Eq. 4.

3 Results and Discussion

The first column in Fig. 3 shows the φ^{tr} of the binary-valued cylindrical structure at SNR = ∞. Below, the noise-contaminated φ^{tr} with added white noise at SNR = 50 is shown.

On the top of the second column, the ground truth conductivity is shown, i.e., the conductivity values of the binary-valued cylinder, while below the conductivity is shown with the marked location of image boundary conditions and collocation points in yellow.

On the third column the numerical reconstructions at SNR = ∞ by std-EPT from Eq. 2 on the top, by stab-EPT from Eq. 3 in the middle, and the numerically estimated Laplacian ($\nabla^2\varphi^{\text{tr}}$) is shown at the bottom.

On the fourth column, the numerical reconstructions at SNR = 50 as well as the numerically estimated Laplacian at the bottom.

To the right, PINN reconstructions and estimated Laplacian are shown without Eq. 5 during training, i.e. boundary conditions and collocation points are not provided during training. Next, PINN reconstructions and estimated Laplacian are shown without Eq. 6 during training, i.e., the residual is not accounted for. Lastly, in the last column, the reconstructions from both methods and corresponding Laplacian from the proposed PINN are shown.

The structural similarity index (SSIM) [13] reconstruction metric is added below each conductivity reconstruction, it is shown that when the PINN with the residual is added the reconstructions show higher similarity to the ground truth conductivity.

Moreover, the PINN estimated, and numerically calculated Laplacian are shown. Laplacian SSIM values are shown compared to the numerically calculated Laplacian at SNR = ∞, it is shown that the estimated Laplacian by the proposed method possesses the highest SSIM value.

Results indicated that the proposed PINN accurately esti-

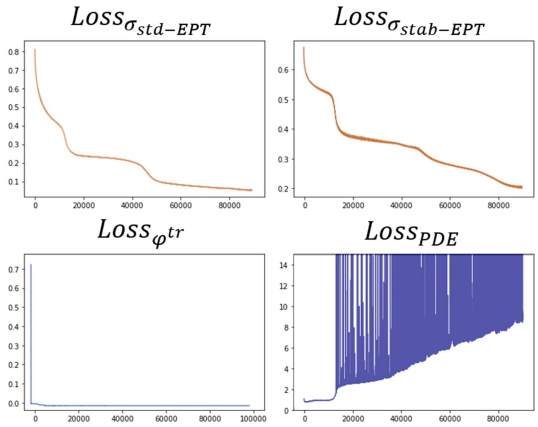

Figure 4. Loss curves during training for the proposed PINN reconstructions method. $Loss_{\varphi^{\text{tr}}}$ shows the sustained accuracy of the predicted $\hat{\varphi}^{\text{tr}}$. $Loss_{\sigma_{std-EPT}}$ and $Loss_{\sigma_{stab-EPT}}$ shows the convergence of the boundary conditions and collocations points according to std-EPT and stab-EPT formulations, respectively. $Loss_{\mathbf{PDE}}$ shows the residual added.

mates partial derivatives for MREPT even in high noise conditions, this can be seen by comparing the Laplacian ($\nabla^2\phi^{\text{tr}}$) calculated numerically in the third column which is highly affected by noise or the Laplacian estimated by PINN on the last column which does not show noise-related artifacts.

The loss curves $Loss_{\varphi^{\text{tr}}}$, $Loss_{\sigma_{std-EPT}}$ and $Loss_{\sigma_{stab-EPT}}$ inf Fig. 4 show the convergence of PINN to the φ^{tr}, the boundary conditions and collocation points. $Loss_{\mathbf{PDE}}$ is shown to increase, nonetheless, it bounds the possible solutions as can be seen by the peaks in the loss curves and the reconstruction results on the last column of Fig. 3.

4 Conclusion

In this work, PINNs are used for the first time in the literature to address the noise sensitivity of MREPT due to numerical differentiation. A training framework with a data-fidelity warm-up mechanism is adopted, and a novel double reconstruction technique is produced to extract further information from the collocation points. This is an initial step to develop a PINN-MREPT to reconstruct conductivity. Future work will focus on including further physical constraints in the form of equations to the residue loss to further reduce the number of collocation points needed.

References

[1] M. Bodenstein, M. David, and K. Markstaller, "Principles of electrical impedance tomography and its clinical application," *Critical Care Medicine*, vol. 37, no. 2, pp. 713–724, 2009.

[2] W. Zhou, P. Wu, W. C. Mu, W. Yu, and S. Huang, "Compact broadband planar resonator with a viaed double spiral for robust wireless power transfer," *IEEE J. Electromagn., RF, Microw. Med. Biol.*, pp. 1–1, 2021.

[3] U. Katscher, C. Findeklee, P. Vernickel, K. Nehrke, T. Voigt, and O. Dössel, "Determination of Electric Conductivity and Local SAR Via B1 Mapping," *IEEE Transactions on Medical Imaging*, vol. 28, no. 9, pp. 1365–1374, 2009.

[4] N. Gurler and Y. Z. Ider, "Gradient-based electrical conductivity imaging using MR phase," *Magnetic Resonance in Medicine*, vol. 77, no. 1, pp. 137–150, 2017.

[5] F. S. Hafalir, O. F. Oran, N. Gurler, and Y. Z. Ider, "Convection-reaction equation based magnetic resonance electrical properties tomography (cr-MREPT)," *IEEE Transactions on Medical Imaging*, vol. 33, no. 3, pp. 777–793, 2014.

[6] C. Li, W. Yu, and S. Y. Huang, "An MR-Based Viscosity-Type Regularization Method for Electrical Property Tomography," *Tomography (Ann Arbor, Mich.)*, vol. 3, no. 1, pp. 50–59, 2017.

[7] D. P. Kingma and J. Ba, "Adam: A method for stochastic optimization," in *3rd International Conference on Learning Representations, ICLR 2015, San Diego, CA, USA, May 7-9, 2015, Conference Track Proceedings*, 2015.

[8] M. Raissi, P. Perdikaris, and G. E. Karniadakis, "Physics-informed neural networks: A deep learning framework for solving forward and inverse problems involving nonlinear partial differential equations," *Journal of Computational Physics*, vol. 378, pp. 686–707, 2019.

[9] G. J. Both, S. Choudhury, P. Sens, and R. Kusters, "DeepMoD: Deep learning for model discovery in noisy data," *Journal of Computational Physics*, vol. 428, p. 109985, 2021.

[10] H. Wen, "Noninvasive quantitative mapping of conductivity and dielectric distributions using RF wave propagation effects in high-field MRI," *Medical Imaging 2003: Physics of Medical Imaging*, vol. 5030, p. 471, 2003.

[11] D. I. Hoult, "The principle of reciprocity in signal strength calculations - A mathematical guide," *Concepts in Magnetic Resonance*, vol. 12, no. 4, pp. 173–187, 2000.

[12] H. J. Kelley, "Gradient theory of optimal flight paths," *Ars Journal*, vol. 30, no. 10, pp. 947–954, 1960.

[13] Z. Wang, A. C. Bovik, H. R. Sheikh, and E. P. Simoncelli, "Image quality assessment: From error visibility to structural similarity," *IEEE Transactions on Image Processing*, vol. 13, no. 4, pp. 600–612, 2004.